Laser Transmitter Design and Performance for the Slope Imaging Multi-polarization Photon-counting Lidar (SIMPL) Instrument

Anthony W. Yu*[a], David J. Harding[b], Philip W. Dabney[a]
[a]NASA Goddard Space Flight Center, Greenbelt, MD, USA 20771

ABSTRACT

The Slope Imaging Multi-polarization Photon-counting Lidar (SIMPL) instrument is a polarimetric, two-color, multi-beam push broom laser altimeter developed through the NASA Earth Science Technology Office Instrument Incubator Program and has been flown successfully on multiple airborne platforms since 2008.[1] In this talk we will discuss the laser transmitter performance and present recent science data collected over the Greenland ice sheet and sea ice in support of the NASA Ice Cloud and land Elevation Satellite 2 (ICESat-2) mission to be launched in 2017.[2]

Keywords: Solid-state laser, Airborne altimetry instrument, Space lidar instrument

1. INTRODUCTION

1.1 SIMPL Instrument

The functional block diagram of the SIMPL instrument is shown in Figure 1(a). The SIMPL instrument is a mono-static design with the transmit and receive signal sharing a common telescope as illustrated in Figure 1(b). It is based on en earlier successfully flown Cloud Physics Lidar (CPL) instrument developed at Goddard Space Flight Center.[3] The SIMPL laser transmitter is a high repetition rate (~11 kHz), short-pulse (~1 ns), linearly polarized microchip laser centered at 1064 nm. Part of the near infrared (NIR) beam at 1064 nm is frequency doubled to 532 nm (Green). Each of the NIR and Green beams is split into four push-broom beams. The output of the SIMPL instrument has 4 linearly polarized beams each with co-aligned wavelengths in order to have co-incident NIR and Green footprints at the surface. The 4-beam, dual color swath spans a width of ~7.2 mrad with equally spaced beams as illustrated in Figure 2. All transmitted beams have the same state of polarization (SOP) when projected to the ground. A 20-cm-diameter off-axis parabola (OAP) is used as the telescope primary to collect the return signal. The OAP permits a rugged and robust design and eliminates most obscurations to both the outgoing and the incoming beams. None of the outgoing transmitted light is lost to obscurations, and only approximately 20% of the receiver aperture is obscured. The return signal collected by the telescope is separated into wavelength components by use of dichroic filter.

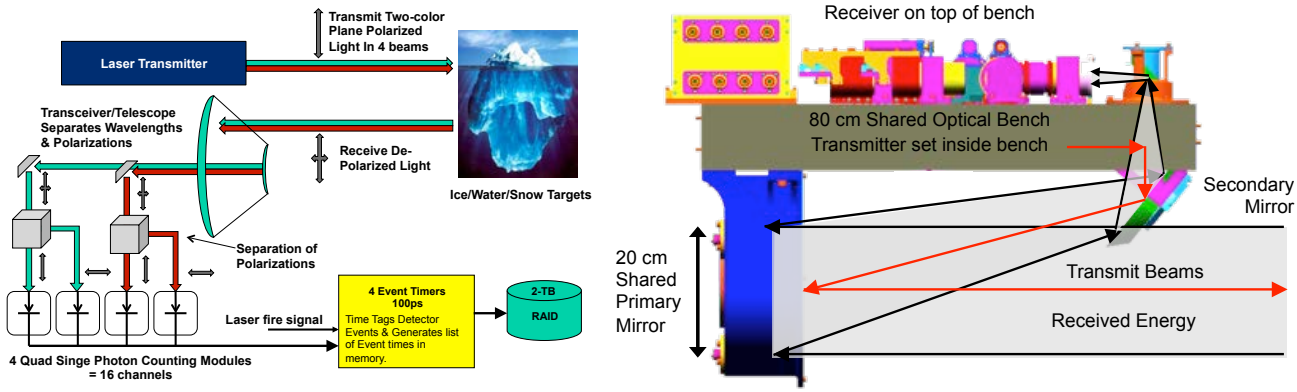

(a) (b)

Figure 1. (a) SIMPL Instrument Functional Block Diagram. (b) The SIMPL instrument transceiver uses an off-axis parabola (OAP) optical design with the transmitter and receiver sharing the optical bench and primary and secondary mirrors. This design provides for stable laser footprint to receiver field of view alignment, co-aligned NIR and green transmit beams and co-incident NIR and green footprints.

*anthony.w.yu@nasa.gov; phone 1 301 614-6248

The receiver dichroic divides the two wavelengths into separate paths which are further divided using polarizing beam splitting cubes into signals parallel and perpendicular to the transmit beam. Sixteen single-photon counting modules (SPCM) and timing electronics with 0.1 nsec precision are used to determine range to the target for the four color/polarization states on the four beams. The short pulse width and high timing precision achieves an 8 cm range precision per single detected photon. Upon aggregation of the signal photons into a range histogram a measurement with a few cm resolution of pulse broadening is achieved. The broadening is due to surface slope and roughness within the footprint and light transmission into the target resulting in volume scattering.

1.2 Instrument Requirements

The SIMPL instrument system requirement and flow-down requirements for the transmitter and receiver subsystems are summarized in Table 1.

Table 1. Summary of the SIMPL instrument system and subsystems requirements.

System Requirements – • 4 cross-track spots illuminated by plane polarized Green (532 nm) and NIR (1064 nm) light • <10 cm single shot range resolution and accuracy • Eye-safe energies at aircraft separation distances (<2,000 ft) • ~0.1 to 0.3 probability of detection (PD) from 8,000 – 16,000 ft Above Ground Level (AGL) • >10 samples / meter in-track	
Laser Requirements -	
Pulse Repetition Frequency (PRF)	11 kHz
Pulse Energy	532 nm: 0.1 to 0.2 µJ per beam; 1064 nm: 0.8 – 1.1 µJ per beam
Wavelengths	532 nm and 1064 nm
Polarization Contrast	>100:1
Pulse Width	< 1 nsec
Output beam pattern	Each color has 4 beam in a line in the cross track direction, full separation: 7.2 mrad, or 2.4 mrad between spots. Each spot divergence ~100 µrad. 532 and 1064 nm beams overlap each other.
Receiver Requirements -	
Photon Detection Efficiency (PDE)	>40% PDE at visible wavelength >3% PDE at 980-1100nm wavelength
Timing error	< 0.33 ns (5cm) single shot
Dark count	< 2 x 10^5/s
Maximum count rate	5-10 x 10^6/s
IFOV (Each beam/Each color)	233 µrad

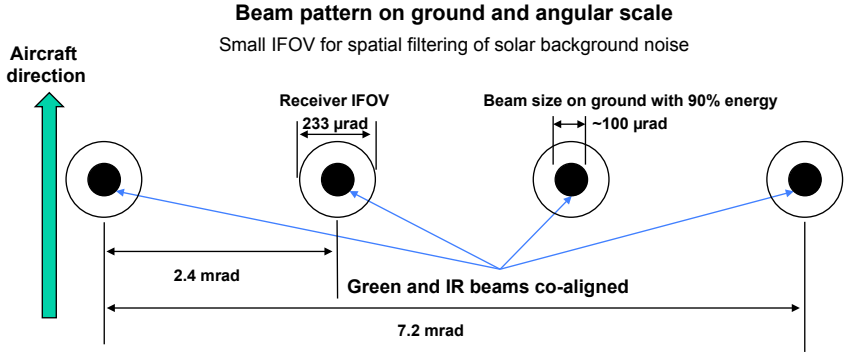

Figure 2. Beam geometry of the output beam for the SIMPL instrument. The dual wavelength beams are co-aligned, spaced equally by ~2.4 mrad spanning a 7.2 mrad swath in a cross track direction. Each beam projects a 100 µrad spot on the ground. The instantaneous filed of view (IFOV) of the received is ~233 µrad per beam. *Note: drawing not to scale.*

The transmit beam geometry of the SIMPL instrument is shown in Figure 2. The swath width is ~7.2 mrad and the four beams are equally spaced with 2.4 mrad spacing. Each beam spot contains both NIR and Green with identical SOP to allow for sampling of the same ground feature.

1.3 SIMPL Laser Transmitter Subsystem

The laser transmitter is a microchip laser, passively Q-switched with pulse repetition frequency (PRF) at ~11 kHz from Teem Photonics (model SNP-08E-OEM) with ~6 µJ of output pulse energy (average power ~70 mW) at 1064 nm. The output beam of the microchip laser is TEM_{00} with a full beam divergence at $1/e^2$ of 12 (Horizontal) x 14 (Vertical) mrad. The laser transmitter layout is shown in Figure 3.

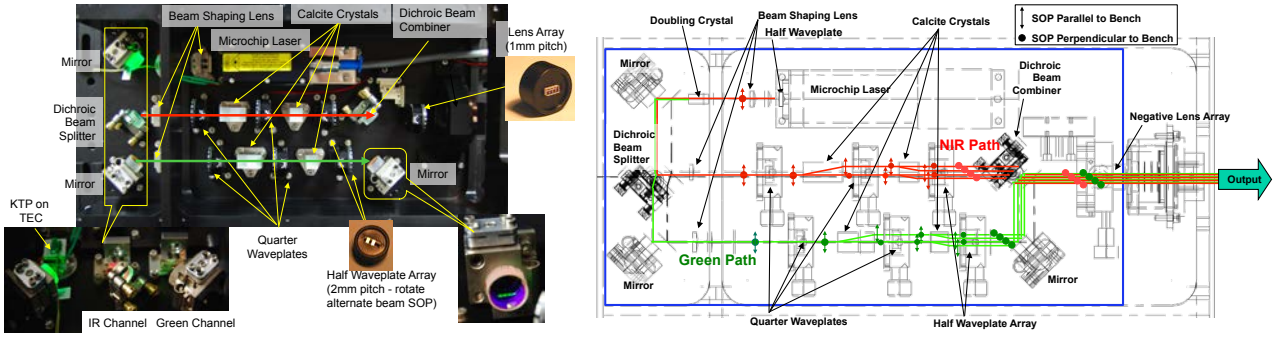

Figure 3. (a) Photograph of the SIMPL laser transmitter showing the separation of the NIR and Green optical paths after the doubling crystal and further separated into the 4 beams per color by use of a dichroic filter and calcite beam separators. The beams are then recombined with a dichroic combiner and co-aligned prior to final beam shaping optics to meet the beam divergence requirement. The lower right hand corner shows the four beams on the green wavelength path prior to recombining with a dichroic beam combiner. (b) The figure shows the polarization beam trace through the system. The output transmit SOP for both colors are perpendicular to the optical bench.

As seen from Figure 3 (a) and (b), a dichroic beam splitter divides the two colors into separate optical paths after the doubling crystal, which followed by beam shaping lenses to establish the beam divergence of ~100 µrad for both colors. After the beam shaping lenses a portion of the energy on each path is reflected vertically and exits the transmitter enclosure through three apertures on the laser transmitter cover. The purpose of these pick-off lights will be described in the Section 1.5. On each optical path a sequence of waveplates and birefringent calcite crystals produce four beams which all have the same polarization plane. The first quarter waveplate circularizes the plane polarized transmit beam which is then split by the first calcite crystal into parallel and perpendicular components forming two beams with equal intensities. The calcite crystal length defines the physical separation of the beams, which is separated by 2 mm. The second quarter waveplate circularizes those beams and then the second, shorter calcite crystal splits the two beams into the two polarization components, forming four beams with equal intensities with a physical pitch of 1 mm between beams. The waveplate array with half waveplates for appropriate wavelengths on a 2 mm pitch rotates the alternate beam polarization planes by 90° so that all beams have the same SOP with the polarization plane oriented perpendicular to the optical bench. A second dichroic beam combiner recombines the two colors and co-aligned the 1064 nm and 532 nm beams. A 4-lens array establishes the 2.4 mrad beam-to-beam divergence. A polarizing beam splitter is used as a final step to ensure ≥ 100:1 polarization contrast ratio.

After passing through the polarizing beam splitter the transmit beams reflect off of a small folding mirror. The folding mirror directs the beams perpendicularly to the secondary mirror that reflects the beams to the 20 cm diameter primary mirror. That mirror reflects the beams at nadir to the surface. Upon exit from the instrument the beams are overlapping with a combined diameter of 70 mm and 5 mm beam-to-beam separation. The nominal ocular hazard distance (NOHD) of the combined beams and colors is 0 m and is therefore eye safe. The diverging beams become fully separated at a distance of 23 m.

1.4 Frequency Doubling

The second harmonic generation (SHG) is done using a Type II non-critically phase matched (NCPM) KTP crystal that is temperature controlled using a thermal electric cooler (TEC). Temperature control of the KTP crystal determines the

doubling efficiency that allows for real-time adjustments of the NIR/Green conversion ratio during the airborne campaign. The SHG conversion efficiency as function of the KTP crystal temperature is shown Figure 4.

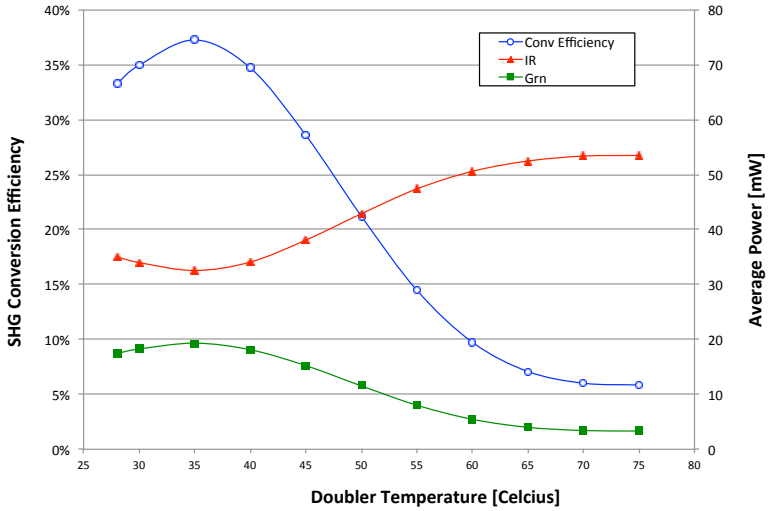

Figure 4. SHG conversion efficiency of the KTP crystal.

1.5 Transmit Echo Pulse, Start Pulse Detector and Power Meter

As mentioned previously, three pick-off optics are placed along different optical paths for monitoring the instrument health as well as to provide critical feature that enhances the instrument functionality. The laser pulse energy directed vertically out of the transmitter enclosure through three apertures is used for three purposes. The first pick-off light enters a start pulse detector to provide pulse events to the receiver electronics that are used as the starting time of the photon round-trip travel time measurement. The other two wavelength paths also have their own pick-off optics for power monitoring and for capturing the transmit echo pulse (TEP). For each wavelength, light enters a beam splitter cube that directs part of the light for power monitoring and a portion of the light is directed to the TEP collection lenses. The TEP optics are used to record the instrument impulse response pulse shape which is the convolution of the transmit pulse shape and the receiver pulse broadening. As seen in Figure 5, individual single mode fibers transmit the energy through couplers to 34 m fiber spools that delay the pulses to separate them in time from internal scattered light signals. The delay fibers are coupled to fibers that transmit the pulses to projection lenses that disperse the light into the primary mirror. This light follows the receive path to record the impulse responses on the sixteen (2 colors x 2 polarization states x 4 beams) single photon counting modules (SPCM) using the same optics and electronics as the pulses reflected from the surface. Deconvolution of the impulse response from the surface return provides a measure of pulse broadening due to surface roughness, slope and penetration.

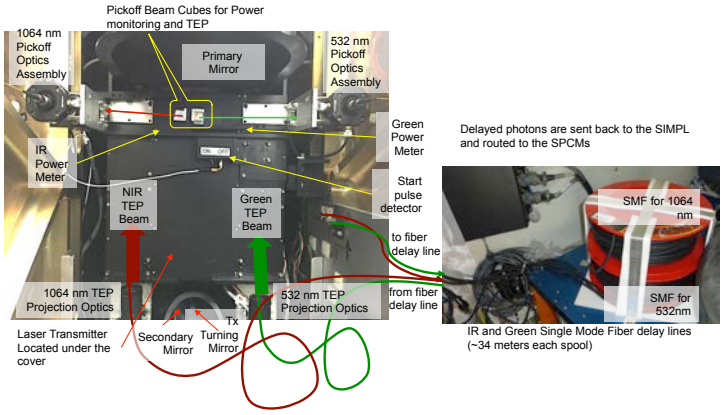

Figure 5. Layout of the pick-off optics for health monitoring and TEP in the SIMPL instrument.

1.6 Receiver Subsystem

The return signal is captured by the instrument's 20 cm OAP aperture, a small portion of the return laser energy is obscured by the secondary mirror assembly. The remaining energy is collected by the primary mirror and then passes through an opening in the optical bench and enters a folding mirror assembly that reflects the light to a pin-hole field stop. The field stop consists of four pinholes that define a 233 µrad field of view for each beam. The small fields of view (FOVs) are used to spatially reject solar background photons. A lens array follows that collimates the incoming beams and a dichroic beam splitter divides the two colors into separate optical paths.

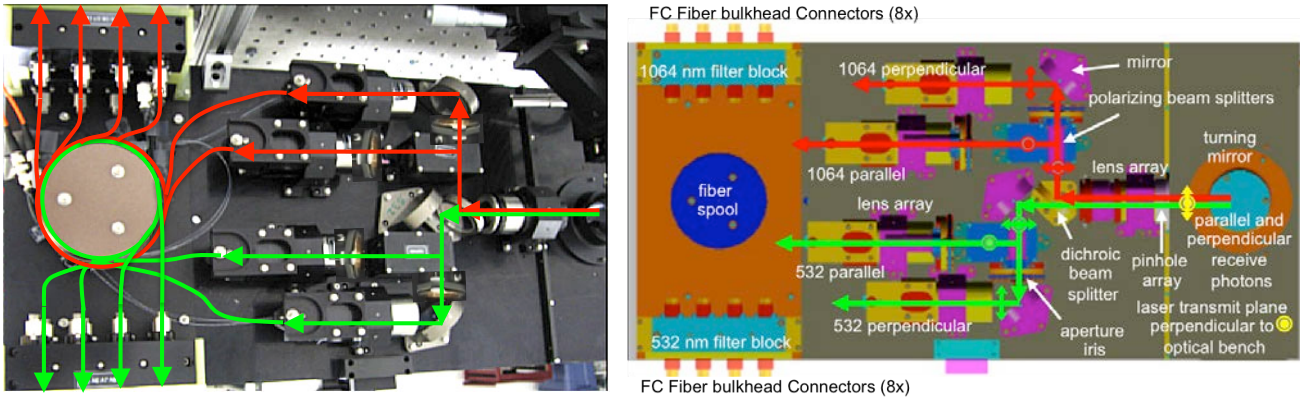

(a) (b)

Figure 6. (a) Photograph of the receiver subsystems, the lines showing the fiber routing paths for the NIR and green signal. (b) Schematic diagram of the receiver subsystem with polarization ray trace through the receiver paths for each color.

As shown in Figure 6, on each path a double stack of polarizing beam splitters separates the return energy into photons with polarization states that are parallel and perpendicular to the plane-parallel polarized transmit beams. The four color and polarization modes each pass through a mechanical iris that can be used to attenuate the beam energy (the irises were not installed on the bench at the time of the photo; insets have been added to show their location). Lens array assemblies for each of the four modes focus the beams into four fibers that have a 0.22 numerical aperture and 100 micron stepped index core size. Using a spool to reduce bending the fibers are coupled to 1064 nm and 532 nm filter blocks each of which consist of eight narrow-band spectral filter assemblies to reject out-of-band solar background photons. The filter assemblies are temperature controlled to maintain stable band pass wavelengths. Four thermistors are installed to record the temperature at two locations on each filter block using a four-channel data logger. On exit from the filter blocks 16 fibers, which have a 0.37 numerical aperture and 200 µm step-index core size, transmit the signals to four SPCM quad detectors in an adjacent instrument rack. The four signals for a beam are directed to one of the quad detector modules. The SPCM detection quantum efficiency is in the range 50 to 60% at 532 nm and 1.6 to 2.3% at 1064 nm. SPCMs were the only photon counting detectors available at the time of SIMPL's development with sensitivity in the NIR.

1.7 Electronics and Command and Data Handling (C&DH)

An electronics rack is used to house an enclosure containing four quad SPCM modules (totaling 16 channels) as seen in Figure 7(a) and (b). The rack also houses a power supply enclosure, dual channel power meter and a doubling crystal temperature controller. The crystal temperature controls the amount of 1064 nm energy doubled to 532 nm. The temperature set point determines the doubling efficiency defining the proportional amount of 164 nm and 532 nm power as shown in Figure 4. The power supply enclosure contains three DC power supplies, a start-pulse discriminator, two 1 to 10 TTL fanout boards and front panel mounted voltage and current meters. The discriminator takes as input the signal laser fire start pulse detector. One fanout board takes this discriminator TTL output and produces duplicate laser fire pulses that go to the four individual SPCM to P7889 event timer interface boards. The other fanout board distributes the GPS 1 pulse per second (pps) signal to the four event timer Interface boards.

The C&DH (shown in Figure 7(c)) rack houses the enclosure containing four P7889 event interface boards. Each board times the arrival of start pulse, GPS pps and photon events with 100 picosecond (1.5 cm) resolution. Each times the

photon events for the four channels on a beam (1064 nm parallel and perpendicular and 532 nm parallel and perpendicular). The relative arrival time of events are defined by the CPU clock frequency. The CPU absolute time is controlled by the GPS pps time provided by a totally accurate clock (TAC) that receives input from a dual-frequency GPS antenna. The computer issues commands to the instrumentation and stores the invent arrival times on RAID drives. The rack also houses CPU keyboard and screen and the laser controller and power supply. A laptop is used to run the Applanix Pos AV and power meter software. It also records the frame camera images.

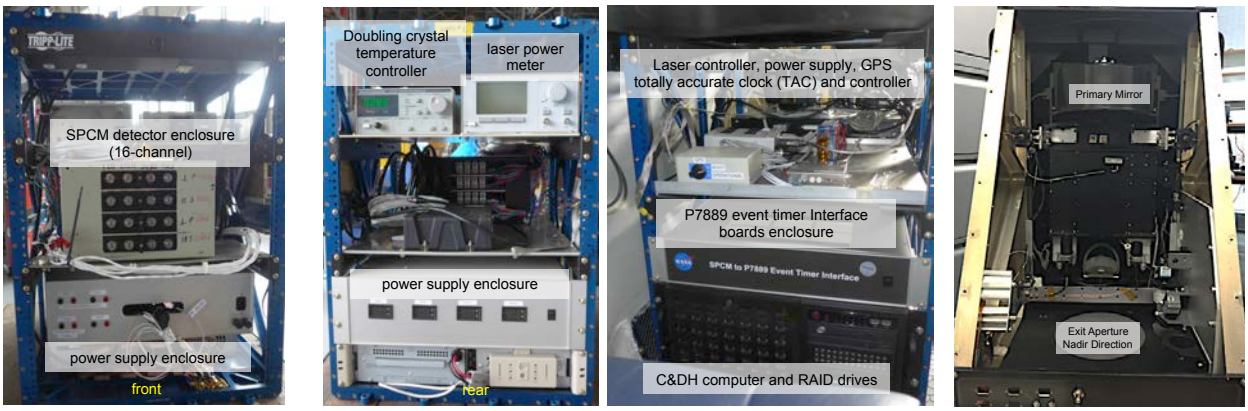

(a) (b) (c) (d)

Figure 7. (a) Front and (b) rear of the electronics rack and (c) C&DH rack for the SIMPL (d) instrument.

2. SIMPL LIDAR PERFORMANCE AND RESULTS

2.1 Measurement technique

SIMPL's measurements provide information about surface elevation, roughness and slope as well as scattering properties used to differentiate surface properties and types. By measuring the depolarization of the plane-polarized transmit pulses at the two wavelengths SIMPL has a unique capability to differentiate surface types, building upon prior non-ranging measurements of laser depolarization at 355, 532 and 1064 nm.[4,5] By adding the ranging component, SIMPL provides a means to investigate the vertical distribution of optical scattering properties to better understand the interaction of pulsed laser energy with surface targets. The depolarization ratio (perpendicular / parallel) is sensitive to the proportions of specular reflection and surface and volume scattering, and is a function of wavelength. Upon single scattering from a surface the reflected energy remains parallel to that of the plane-polarized laser pulse. As multiple scattering increases the fraction of the energy converted to the perpendicular state increases, as does the depolarization ratio. Prior work using data acquired over Lake Erie ice cover demonstrated differentiation of open water, snow and several ice facies as well as differences in the depth of laser pulse penetration,[6] results of relevance for planned ICESat-2 measurements of sea ice thickness.[7] For canopies, the degree of depolarization is a function of wavelength and the reflectance phase function, transmission, size and spacing of foliage and woody components and the specular character of waxy broadleaf coatings, if present.[5] Ground depolarization is a function of wavelength, the type of ground-cover and its retro-reflectance and roughness.

2.2 airborne campaign

The SIMPL instrument has been successfully flown on a few airborne campaigns since 2010. Most recently an airborne campaign was completed to support the NASA's upcoming ICESat-2 mission. The primary objective of the ICESat-2 mission is to collect altimetry data of the Earth's surface optimized to measure ice sheet elevation change and sea ice thickness.[2] The mission's multi-beam, photon-counting lidar, ATLAS, will collect that data. Understanding ranging biases in the altimetry measurements for snow, ice and water is needed to quantify errors in the elevation data for those surfaces. One potential source of bias is penetration of ATLAS's 532 nm (green) laser pulses into those materials with the associated volume multiple-scattering introducing photon path delays. Changes in penetration depth due to seasonal and/or inter-annual changes in snow and ice optical properties could result in small errors in the trends of ice sheet elevation change. Penetration differences into sea ice versus open water could introduce errors in sea ice freeboard

measurements that are the basis for determination of sea ice thickness.

To study this issue of penetration bias the airborne SIMPL instrument acquired ice sheet and sea ice data based at Thule Air Force Base in Greenland during July and August 2015. The 1064 nm photons provide a reference to the true surface elevation because the penetration depth is negligible at that wavelength. The co-incident wavelengths illuminate small footprints (30 cm diameter) so that return pulse broadening due to surface slope and roughness is minimized in order to observe the broadening due to penetration. Eight cm single photon range precision enables sub-cm level determination of penetration depth using calibrated range histograms. SIMPL's measurement of laser return depolarization uniquely identifies the presence of surface water, aiding in the interpretation of the penetration results. In order to examine ice sheet penetration biases as a function of surface conditions data was acquired for higher-altitude, interior dry snow as well as western coastal ablation zone ice and melt ponds. Data for multi-year sea ice with open leads was acquired north of Greenland.

Sample altimetry data captured using the SIMPL instrument on a melt pond is shown in Figure 8(a) for 532 nm and Figure 8(b) for 1064 nm. The data clearly showed the penetration of the 532 nm light penetrating into the melt pond while none for 1064 nm light.

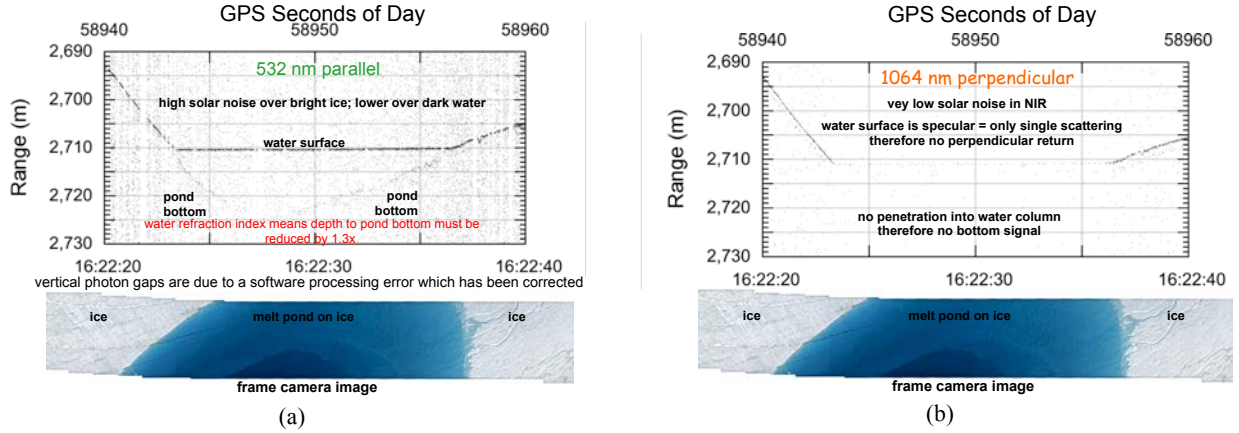

Figure 8. Sample altimetry data for (a) 532 nm parallel SOP and (b) 1064 nm perpendicular SOP from SIMPL at a Melt Pond on Ablation Zone Ice. Camera image of the sampled area is shown below each data set.

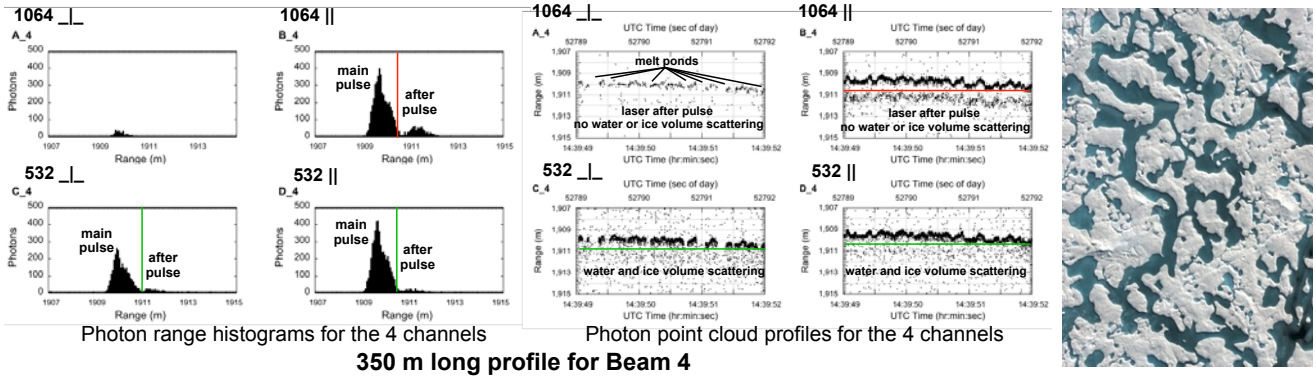

Figure 9. Data showing the perpendicular (_|_) and parallel (||) components of the NIR and green returned signal for one of the 4 beams of the 4-beam track. The image on the right shows Nares Strait Pack Ice with Melt Pond Network.

In Figure 9, the captured data near the Nares Strait pack ice with melt pond network showed the absence of NIR and green perpendicular signals identifies the location of melt ponds. The low signal strength from the ice for 1064 nm

perpendicular (_|_) is because NIR multiple scattering is rare and the stronger 532 nm _|_ ice signal is because green multiple scattering is more frequent. The histogram shapes are broadened due to surface slope and roughness. The surface slope is due to aircraft roll effect, which is not removed in this range data. The 532 nm penetration into ice and water is seen in the volume scattering below the surface where the photon density is higher than the background noise.

3. CONCLUSIONS

SIMPL lidar was developed under the NASA Earth Science Technology Office (ESTO) Instrument Incubator Program (IIP) in 2004. Since 2013, a series of airborne campaigns was successfully executed and valuable data on depolarization due to ground feature types have been studied and documented. The airborne four-beam SIMPL instrument is ideally suited to quantify green laser pulse penetration depths into snow, ice and water. It also definitely identifies the presence and depth of melt ponds on ice sheets and sea ice from the nine science flights during July and August, 2015 in northwest Greenland, totaling 37 hours, collected data for a wide range of surface types in support of NASA's ICESat-2 mission, which is scheduled to launch in late 2017.

The authors acknowledge the support from NASA's ESTO and ICESat-2 mission office.

REFERENCES

[1]. Harding, D.J., J.B. Abshire, P.W. Dabney, T.A. Scambos, A.A. Seas, C.A. Shuman, X. Sun, "The Swath Imaging Multi-polarization Photon-counting Lidar (SIMPL): A Technology Demonstration for Space-based Laser Altimeter Swath Mapping," URL: http://esto.nasa.gov/conferences/nstc2007/papers/Harding_David_B7P4_NSTC-07-0150.pdf, NASA Science Technology Conference (NSTC2007), 19-21 June 2007.

[2]. http://icesat.gsfc.nasa.gov/icesat2/

[3]. McGill, M., D. Hlavka, W. Hart, V. S. Scott, J. Spinhirne and B. Schmid, "Cloud Physics Lidar: instrument description and initial measurement results," Applied Optics, 41, 18, 3725-3734 (2002).

[4]. Kalshoven, Jr., J.E. and P.W. Dabney, "Remote sensing of the Earth's surface using an airborne polarized laser," IEEE Trans. Geosci. Remote Sensing, 31, 438–446 (1993).

[5]. Kalshoven, Jr., J.E., M.R. Tierney, Jr., C.S. T. Daughtry and J.E. McMurtrey III, "Remote sensing of crop parameters with a polarized, frequency-doubled Nd:YAG laser," Appl. Opt., 34, 2745- 2749 (1995).

[6]. Dabney, P., D. Harding, J. Abshire, T. Huss, G. Jodor, R. Machan, J. Marzouk, K. Rush, A. Seas, C. Shuman, X. Sun, S. Valett, A. Vasilyev, A. Yu, and Y. Zheng, "The Slope Imaging Multi-polarization Photon-counting Lidar: development and performance results," Proc. Int. Geosci. Rem. Sens. Symp., 11686732, DOI 10.1109/IGARSS.2010.5650862, 253-256 (2010).

[7]. Abdalati, W., H.J. Zwally, R, Bindschadler, B, Csatho, S.L. Farrell, H.A. Fricker, D. Harding, R. Kwok, M. Lefsky, T. Markus, A. Marshak, T. Neumann, S. Palm, B. Schutz, B. Smith, J. Spinhirne and C. Webb, "The ICESat-2 laser altimetry mission," Proc. IEEE 98(5), 735-751 (2010).